SURFACE STUDIES OF ELECTRODES USED IN SPARK GAPS*

G. Jackson, L. Hatfield
Department of Physics

M. Kristiansen, M. Hagler, A.L. Donaldson, R. Ness
Department of Electrical Engineering
and
J. Marx
Department of Chemistry
Texas Tech University
Lubbock, Texas 79409

ABSTRACT

Protrusions on the surfaces of electrodes used in high voltage spark gaps lead to local field enhancements, which lower the self-breakdown voltage of the spark gap. Stainless steel, brass, and copper-tungsten electrodes have been tested in a 5-30 kV, 4-25 kA, .1-.6 Coul/shot, unipolar, pulsed spark gap with N_2 gas or air. The heights and bases of variously shaped protrusions on the surfaces of these electrodes have been measured using stereo pair micrographs from a Scanning Electron Microscope. For instance, a brass electrode exposed to 5000 shots in N_2 has a large number of irregularly shaped protrusions on its surface with base diameters ranging in size from 100 μ to 1000 μ and heights ranging in size from 250 μ to 500 μ. Consequently, the self-breakdown voltage statistics for brass electrodes have a very erratic shape. The composition of these protrusions has been determined using Auger Electron Spectroscopy. They are composed of a much larger ratio of copper to tin than is normally observed in brass.

INTRODUCTION

The purpose of this study is to investigate the chemical and physical processes that occur on the surfaces of electrode materials used in a high energy, gas filled, spark gap. Protrusions on the surfaces of electrodes, resulting from erosion processes, lead to local field enhancements on the surface, which may lower the self-breakdown voltage of the spark gap.[1] The size, shape, and distribution of these protrusions will determine the distribution of local field enhancements, and the chemical composition of these protrusions will influence processes such as field emission and thermionic emission which produce initial electrons in the gap. If these initial electrons are born at a site of local field enhancement the self-breakdown voltage of the gap may be very low.

In order to study these protrusions a Scanning Electron Microscope (SEM), an Auger Electron Spectrometer (AES), and an optical microscope were used. Stereo pairs of protrusions were taken with the SEM and examined with a stereo viewer in order to obtain information about their height, shape and distribution on the surface. AES was used to determine the composition of these protrusions and the composition of the substrate material on which these protrusions are located.

EXPERIMENTAL SETUP:

The spark gap shown schematically in Figure 1 was used to test the various electrode materials in different gases. The electrode materials tested were 304 stainless steel, and a tungsten-copper composite (K33). Air and nitrogen were the two gases used in these studies. This spark gap is designed for frequent electrode and insulator replacement and to allow for accurate control of the electrode alignment and gap spacing. The electrodes are 2.5 cm diameter, hemispherically shaped inserts in a brass holder. The insulator inserts provide protection for the main gap housing and studies of the surfaces of these insulator inserts give information about the debris which is deposited on them as well as information about the effects of the byproducts of the discharges on the insulators.

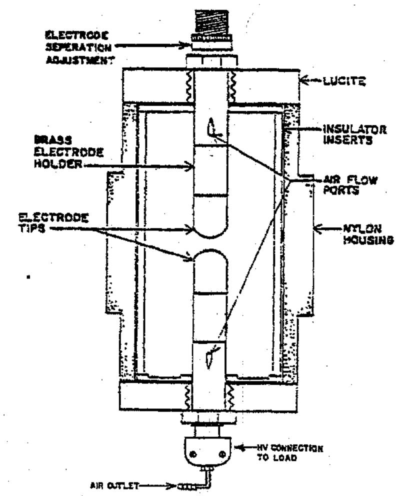

Figure 1 Spark gap used to test different electrode materials in flowing air and nitrogen.

A detailed description of the spark gap assembly and diagnostic system is given in another paper[2], however, the operating parameters of the gap are summarized below.

Operating Conditions

Voltage:	<30 kV
Current:	<25 kA
Total Capacitance:	21 μF
Charge/shot:	<.6 C
Energy/shot:	< 9 kJ
Pulse width:	25 μs
Rep-rate:	< 5 pps
Pressure:	1 atm (absolute)
Flow rate:	1 gap volume every 5 sec.
Gap spacing:	<.75 cm

The analysis of the electrodes was performed with a PHl model 595 Auger Electron Spectrometer, a JEOL JSM-2 Scanning Electron Microscope and an optical microscope.

RESULTS

Virgin samples of 304 stainless steel and K-33 were analyzed using AES in order to make a comparison between an untreated electrode and electrodes used in this spark gap. Initial analysis of these materials showed that they were covered with a thin layer of carbon and oxygen. The stainless steel sample surface was composed of carbon (67%), oxygen (22%), and iron (11%). A virgin K-33 sample exhibited a surface com-

*Supported by AFOSR

posed of carbon (30%), oxygen (7%), copper (13%) and tungsten (50%). These samples were then etched with a 5 kV Argon ion beam in order to remove this top layer. After sputtering for 120 seconds the AES scan showed that the stainless steel sample surface was composed of carbon (2%), oxygen (2%), iron (67%), chromium (21%), and nickel (7%), whereas the known bulk concentration of this alloy is iron (70.2%), chromium (22%), and nickel (9.3%). After sputtering for 30 seconds the AES scan showed that the K-33 sample surface was composed of copper (28%) and tungsten (72%), whereas the known bulk concentration of this alloy is copper (33%) and tungsten (66%).

This kind of layer on the electrodes is typical and is assumed to be the result of exposure of the electrode, after it has been machined, polished, and cleaned, to the ambient laboratory atmosphere. Hydrocarbons which could produce such a layer are always present in the air. This contaminated surface could explain why the self-breakdown voltage of the spark gap is higher for the first few shots during a sample run. During these shots the electrodes are being conditioned by the discharges which remove this hydrocarbon layer from the surface, and expose the bulk material underneath. However, the material which is removed from the surface and decomposed during these shots, can be redeposited onto the electrodes once a discharge is complete. Consequently, the surface may always exhibit a contaminated layer.

A stainless steel cathode used in this gap, with 1 atmosphere absolute pressure of flowing nitrogen gas, was removed after 2000 shots and visually inspected with the naked eye. There were three distinct circular regions on the electrode surface. The inner region, the center portion of the electrode, was approximately 14 mm in diameter and very rough in appearance. Figure 2 is an SEM micrograph of this region at a magnification of 400. The two areas marked 7 and 8 were analyzed with AES. The area marked 7 in this micrograph had a surface composition of carbon (41%), oxygen (38%), nitrogen (4%), and iron (17%). After sputtering for 30 seconds the composition was carbon (0%), oxygen (30%), nitrogen (17%), chromium (26%), iron (22%), and nickel (5%). The area marked 8 in this micrograph had a surface composition of carbon (47%), oxygen (28%), nitrogen (7%), chromium (5%), iron (11%) and nickel (3%) but after sputtering for 30 seconds it changed to carbon (7%), oxygen (21%), nitrogen (12%), chromium (20%), iron (35%), and nickel (6%). This protrusion on the surface has a diameter of about 100 μm and a height of about 62 μm. It is difficult to determine whether the carbon and oxygen on the surface are from exposure to air after removal from the spark gap or from contamination in the system. Further analysis of this electrode with AES indicates that the majority of the oxygen seen on the surface is "tied up" in bonds with the iron.

The second ring of this electrode is only about 2 mm in width and fairly smooth in appearance. Figure 3 is an SEM micrograph of this surface at a magnification of 1000. Obviously this region has fewer gross features than the inner region shown in Figure 2 (the heights of protrusions on this surface are no larger than 10 μm). The surface composition of this region was carbon (34%), oxygen (43%), nitrogen (2%) and iron (21%). After sputtering the composition was carbon (6%), oxygen (46%), nitrogen (9%), iron (31%), chromium (4%) and nickel (5%). The oxygen appears to be bonded with the iron and the stoichiometry indicates a compound, possibly of the form Fe_2O_3.

The outermost ring on this electrode covered much of the remainder of the electrode surface. Analysis of this region with AES was not possible due to surface charging. These surface charging problems are common in AES, when the surface is covered with an insulating layer.

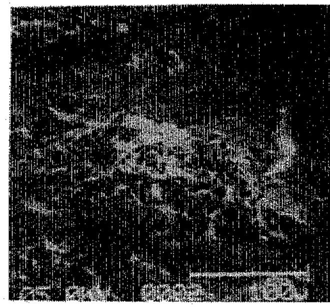

Figure 2 SEM micrograph of the inner region of a stainless steel electrode used in nitrogen.

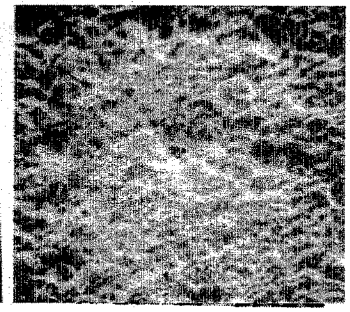

Figure 3 SEM micrograph of middle ring of a stainless steel electrode used in nitrogen.

A stainless steel cathode used in this gap, with 1 atmosphere absolute pressure of flowing air, was removed after 2000 shots and visually examined. This electrode had only two distinct regions of interest and only the center region was examined with AES. Figure 4 is an SEM micrograph of this inner region at a magnification of 240. The surface of this electrode is much smoother in appearance than the stainless steel electrode used in the nitrogen atmosphere. The large particle seems to be imbedded in the surface and has a height of about 32 μm. The density of particles on this surface is only about 1 per mm^2. Another major difference between this electrode and the one used in nitrogen is the platelet like structures seen on the surface. This appears to be material which has redeposited (from a vapor state or a molten state) onto the electrode and drawn together into patches upon cooling. Cross-sectional views of this area indicate that the depth of the valleys between these structures is approximately 50 μm. Auger analysis of this area shows a composition of carbon (15%), oxygen (57%), and iron (29%). After 60 seconds of sputtering the composition was carbon (0%), oxygen (57%), iron (32%), chromium (6%), and nickel (4%), with the iron and oxygen bonded together to form an oxide. The surface composition of the particle is about the same as that of the substrate except that there is a small percentage (4%) of nickel seen in the spectrum before sputtering.

Figure 5 is an SEM micrograph of a K-33 electrode used in this spark gap, with 1 atmosphere absolute of flowing nitrogen. The surface of this electrode is very smooth and similar in appearance to the polished virgin electrode. Visual inspection of this surface indicates only a very small region where actual damage can be seen. AES analysis of this damaged region shows the surface to be composed of carbon (23%), oxygen (15%), nitrogen (5%), copper (34%), and tungsten (23%). After sputtering this surface the AES analysis shows the surface to be composed of tungsten (62%) and copper (38%), which is very nearly the known bulk concentrations of K-33.

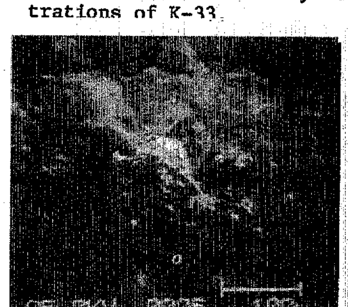

Figure 4 SEM micrograph of the inner region of a stainless steel electrode used in air.

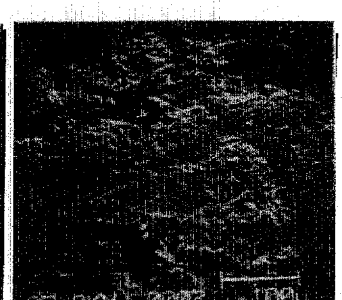

Figure 5 SEM micrograph of a K-33 electrode used in nitrogen.

A K-33 electrode used in this spark gap, with 1 atmosphere absolute pressure of flowing air, for 2000 shots had three distinct regions. The inner region is about 12 mm in diameter and fairly rough looking. The middle ring is about 3 mm in width and appears to be smooth, and finally the outermost region which takes up the remainder of the electrode surface is very black and rough. Figure 6 is an SEM micrograph of the inner region at a magnification of 200. The surface of this electrode is rough and cracked but there are no large protrusions on the surface. Analysis of this area with AES shows that the surface is composed of chlorine (6%), carbon (40%), oxygen (31%), copper (23%), and tungsten (46%).

Figure 7 is an SEM micrograph of the middle ring of this electrode. This area has a completely different appearance from the central region of the electrode. There are a lot of "globs" on this region and the substrate material is very smooth in comparison to the center region. Figure 8 is an SEM micrograph of this area at a magnification of 1000. Auger analysis of the area marked by 1 in this micrograph shows the surface to be composed of carbon (49%), oxygen (16%), and copper (35%). Auger analysis of the area marked by 2 in this micrograph shows the substrate material to be composed of carbon (42%), oxygen (15%), and copper (43%). Sputtering this surface for 30 seconds shows that region 2 is composed of carbon (5%), oxygen (35%), copper (24%), and tungsten (36%). The area in region 1 is composed of oxygen (44%) and tungsten (56%) after sputtering. Apparently, this entire middle ring is covered with a thin layer of copper, which may have condensed from the vapor. However, the "globs" are a tungsten oxide which has resolidified onto a substrate which appears to be unchanged by the discharge.

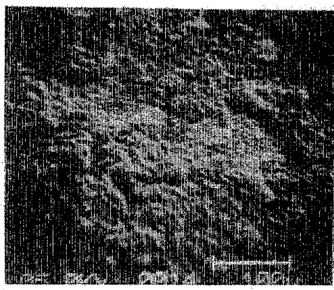

Figure 6 SEM mcirograph of the inner region of a K-33 electrode used in air.

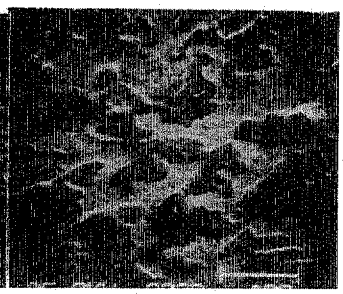

Figure 7 SEM micrograph of the middle region of a K-33 electrode used in air.

Figure 9 is an SEM micrograph of the outermost region of this electrode. The "globs" in this region are much larger than those in the middle ring but they are very similar to the "globs" in the middle ring. For example, Auger analysis of the area enclosed by the square shows the surface to be composed of copper (26%), oxygen (30%) and carbon (44%). Sputtering this surface for 30 seconds shows the surface to be composed of oxygen (24%), copper (24%), and tungsten (52%). The substrate material, on which these "globs" rest, was impossible to analysis with AES due to surface charging.

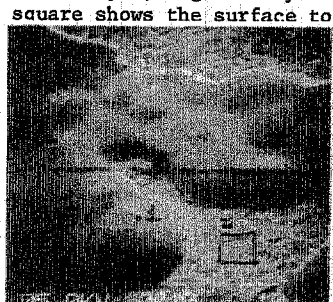

Figure 8 SEM micrograph of the middle region of a K-33 electrode used in air.

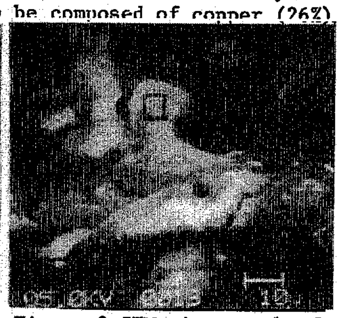

Figure 9 SEM micrograph of the outer region of a K-33 electrode used in air.

A brass electrode used in this gap, with 1 atmosphere absolute pressure of flowing nitrogen gas, was removed after 2000 shots and visually inspected with the naked eye. The surface of this electrode was very rough. SEM micrographs of this surface show that the entire electrode surface is covered with very large irregularly shaped protrusions. The base diameters of these protrusions range in size from 100 μ to 500 μ. Analysis of this surface with AES is very difficult to perform because of the large changes in topography of the surface. The analysis of some of the protrusions on this surface with AES show that these protrusions are composed of carbon (23%), tin (2.1%), oxygen (35%), and copper (36%). After sputtering for 5 minutes the surface of these protrusions is composed of carbon (29%), tin (3%), oxygen (31%), and copper (35%). The copper on this surface is almost completely oxidized even after the surface has been sputtered. This implie that the copper oxide layer on these protrusions is at least 1000 A thick. The self breakdown voltage distribution for these experiments is very difficult to obtain, because after only a hundred or so shots the distribution becomes very erratic.

DISCUSSION OF RESULTS

The self-breakdown voltage of a spark gap is influenced by the type and pressure of gas in the gap, the size and shape of protrusions on the surfaces, the emissivity of the surface, the rate of change of the applied electric field, the temperature of the electrodes, and the spacing of the gap.[3] The self-breakdown voltage distributions for the two different electrode materials studied (stainless steel and K-33) in the two gases (air and nitrogen) are shown in Figures 10-13.

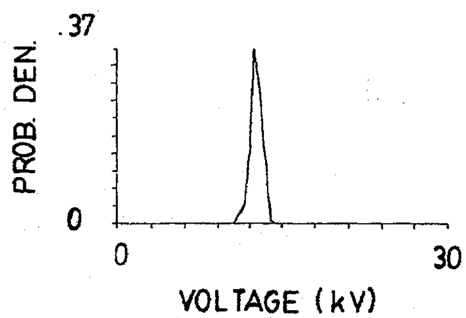

Figure 10 Self-breakdown voltage distribution for a stainless steel electrode in flowing nitrogen (mean = 13 kV, standard deviation = .5 kV)

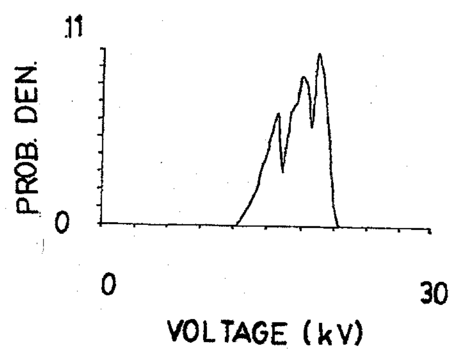

Figure 11 Self-breakdown voltage distribution for a stainless steel electrode in flowing air. (mean = 18 kV, standard deviation = 2 kV)

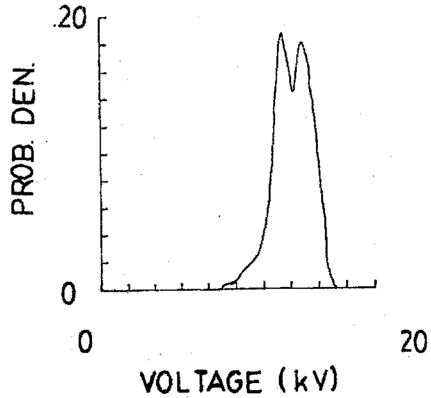

Figure 12 Self-breakdown voltage distribution for a K-33 electrode in flowing nitrogen. (mean = 14 kV, standard deviation = 2 kV)

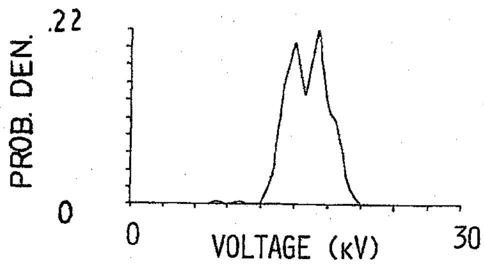

Figure 13 Self-breakdown voltage distribution for a K-33 electrode in flowing air. (mean = 16 kV, standard deviation = 2 kV)

At a pressure of 1 atmosphere absolute the height of a protrusion on the surface of an electrode, which would locally enhance the electric field enough to initiate a breakdown, would have to be greater than 500 μm . Since the heights of protrusions on these surfaces are only about 100 μm, the deviations in the self-breakdown voltage appear to be the result of some other mechanism besides local field enhancements.

The electron emissivity of a surface depends on the work function of the surface, the temperature of the surface, and the applied electric field. In these experiments the type of gas and the pressure are always the same for the different electrodes. The rate of change of the applied electric field and the geometry of the gap are also the same for each run. The emissivity of the surface could be the major factor which determines the self-breakdown voltage distribution.

Analysis of these electrodes with AES indicates that each of these surfaces is covered with some sort of oxide layer or in the case of stainless steel electrodes in nitrogen the surface also exhibits some form of nitride. These different surface layers have different work functions and consequently the emissivity of the surfaces is different. Apparently, the best combination of materials to use, if a narrow self-breakdown voltage distribution is desired, is stainless steel in a nitrogen atmosphere. This narrow distribution may be due to the nitride coatings. For the other electrode and gas combinations the self-breakdown voltage distributions are not much different and thus the oxides must have similiar emmissivities.

REFERENCES

[1] Avrutskii, V.A., Sov. Phys. Tech. Phys. 18, 389(1973)

[2] A.L. Donaldson, "Electrode Erosion Measurements in a High Energy Spark Gap", Master's Thesis, Texas Tech University, 1982.

[3] A.L. Donaldson, R. Ness, M. Hagler, M. Kristiansen, L.L. Hatfield, "Modeling of Spark Gap Performance", Proc. of the IVth IEEE Pulsed Power Conference, Albuquerque, NM, 1983.

ACKNOWLEDGEMENTS

We would like to thank the Air Force Office of Scientific Research for supporting this work. We would also like to thank the Center for Research in Surface Science and Submicron Analysis at Montana State University for the use of their facilities.